Astron. Astrophys. 153, 71–78 (1985)

ASTRONOMY AND ASTROPHYSICS

Radial velocities along the light curve of the peculiar emission-line star GG Carinae*

E. Gosset [1,], D. Hutsemékers [1,***], J. Surdej [2,§], J.P. Swings [1,§§]**

[1] Institut d'Astrophysique, Université de Liège, B-4200 Cointe-Ougrée, Belgium
[2] European Southern Observatory, Karl-Schwarzschild-Strasse 2, D-8046 Garching bei München, Federal Republic of Germany

Received May 13, accepted July 1, 1985

Summary. Measurements of the radial velocities of several emission and absorption lines in a large series of high dispersion spectra of the peculiar emission-line object GG Carinae are combined with the photometric data described by Gosset et al. (1984) in an attempt to derive constraints on a qualitative physical model of this peculiar, and most probably binary, object. Previously unreported spectral features are the double absorption components of the Balmer lines and the He I absorption lines appearing around phase $\phi = 0.45$ of the 31.02 day period deduced from the radial velocity curve.

Key words: radial velocities – stars: emission-line – stars: variable

1. Introduction

At the end of the 19th century, GG Carinae [1] was already known to be a peculiar star showing a spectrum with bright emission lines (Pickering, 1896a, b; Cannon, 1915). Fairly low resolution spectroscopic observations by Smith (1955), by Carlson (1968), and by Carlson and Henize (1979) suggested that GG Carinae was a Bep-type star. Higher resolution data definitely revealed a P Cygni line profile at H_γ, as well as many emission lines of both Fe II and [Fe II] (Swings, 1974). It should also be mentioned that GG Carinae is well known to have an infrared excess of the type believed to originate in a circumstellar dust shell (Allen, 1973; Cohen and Barlow, 1980; Bouchet and Swings, 1982).

The light variability of GG Carinae has interested various astrophysicists (Kruytbosch, 1930; Hoffleit, 1933; Greenstein, 1938; Gaposchkin, 1953; Chen et al., 1983). Nevertheless, the first extensive sets of photoelectric photometry in both the standard *UBV* and Strömgren systems were obtained from 1977 to 1981 (Gosset et al., 1984). Fourier analysis of these leads to the redetermination of the period for the light variation i.e. $P = 31^d.020$. Because of different physical arguments, however, these authors suggested that the true period of the star could be $P = 62^d.039$ i.e. the double. These data would then suggest a possible similarity with β Lyrae-type systems.

Hernandez et al. (1981) were the first to investigate the possible periodic variability of the spectrum of GG Carinae. They mainly reported that the radial velocities of the hydrogen absorptions exhibited a trend better marked in a 31-day phase diagram rather than in a 62-day one. From the H lines, Hernandez et al. (1981) derived the following orbital elements:

$P = 31.030$ d (estimated) for the period;
$K = 45$ or 66 km s^{-1} for the semi-amplitude of the variation;
$e = 0.67$ or 0.47 for the eccentricity.

However, the heterogeneity of their set of spectrograms as well as their "a priori" knowledge of a period for the light variability (Kruytbosch, 1930) led Gosset et al. (1984) to cast some doubt on their conclusions.

The aim of this paper is to present and analyse a set of higher dispersion spectrograms that is more homogeneous in order to solve this problem and, as a consequence, to attempt to refine the model of the object.

2. The spectrum of GG Carinae

It is not the motivation of this section to give a detailed description of the spectrum of this peculiar star, but rather to point out its major characteristics on the basis of the existing publications.

It is clear that, from the low resolution spectrogram described by Smith (1955) and from that described by Carlson (1968) and Carlson and Henize (1979), the only lines that appear in the spectrum of GG Carinae are in emission: from H_β to H_8, Fe II multiplets, no He I except perhaps λ5876 in the former; from H_α to H_{10}, Fe II dominating the spectrum, [Fe II] λ4287, moderately strong λ5876 He I and weak λ4471 He I, plus a few Si II lines in the latter. Carlson and Henize (1979) give radial velocities for these lines, but only for one spectrogram.

On the basis of 12 Å/mm plates, Swings (1974) detected that hydrogen lines had marked P Cygni profiles and that Fe II emission

Send offprint requests to: E. Gosset

* Based on observations collected at the European Southern Observatory, La Silla, Chile

** Chercheur, Fonds de la Recherche Fondamentale Collective, Belgium

*** Aspirant au Fonds National de la Recherche Scientifique, Belgium

§ Also, Chercheur Qualifié au Fonds National de la Recherche Scientifique, Belgium

§§ Associate, European Southern Observatory

1 = CPD-59°2855 = CD-59°3425 = HD 94878 = MWC 215 = Wra 691 = He 3-526

Table 1. *Spectra of* GG *Carinae.* Note: FD = F. Dossin, MK = M. Klutz, AS = A. Surdej, JS = J. Surdej, JPS = J. P. Swings

Plate no.	Year	Month	Day	Phase	Observer	Exposure time (min)
G 6597	1975	03	18	0.958	FD	62
G 7433	1976	03	10	0.499	JPS	54
G 7444	1976	03	14	0.628	JPS	61
G 7455	1976	03	15	0.660	JPS	66
G 7458	1976	03	16	0.693	JPS	72
G 8132	1977	02	03	0.138	MK	60
G 8138	1977	02	06	0.234	MK	55
G 9057	1977	12	29	0.744	AS	114
G 9269	1978	03	27	0.581	JS	96
G 9281	1978	03	29	0.645	MK	123
G 9284	1978	03	30	0.677	MK	112
G 9287	1978	03	31	0.710	MK	197
G 9821	1978	12	23	0.317	JPS	50
G 9869	1979	01	09	0.865	JPS	82
G 9922	1979	01	12	0.962	JPS	73
G 9935	1979	01	11	0.930	JPS	66
G 9982	1979	01	15	0.059	JPS	89
G 10013	1979	01	18	0.155	JPS	75
G 10028	1979	01	20	0.220	JPS	57
G 10074	1979	02	10	0.987	JPS	74
G 10255	1979	03	06	0.670	JPS	90
G 10922	1979	12	04	0.471	JPS	85
G 10928	1979	12	06	0.536	JPS	45

lines appeared double ($\Delta v \sim 30\,\mathrm{km\,s^{-1}}$), whereas [Fe II] λ4287 remained sharper and single. Swings (1974) actually showed that there existed interesting similarities in the spectra of three southern peculiar emission-line stars with infrared excess: HD 45677, HD 87643 and GG Carinae.

Hernandez et al. (1981) describe their 42.0, 29.6, and 49.3 Å/mm spectrograms as follows: H is present from H_α to H_{21} with Beals type III P Cygni profiles; many Fe II lines are present in addition to those of [Fe II] (λ4359 and doubtful $\lambda\lambda$4287, 4452), He I $\lambda\lambda$4471, 5876 also in emission, Si II, perhaps Mg II. Interstellar absorption Ca II K is visible with a velocity of $-23\,\mathrm{km\,s^{-1}}$.

It should also be mentioned that Garrison et al. (1977, 1983) reported the presence in January 1970 of inverse P Cygni profiles for the Balmer lines of GG Carinae: we had the opportunity to reexamine their plates, and noticed that Garrison et al. (1977, 1983) had actually been misled.

3. Observations

The spectrograms examined here were all obtained on baked IIa-O plates at the coudé focus of the European Southern Observatory (La Silla, Chile) 1.52 m telescope: the dispersion was 12.3 Å/mm. Table 1 lists the plates selected for the analysis. A print of most of the plates of Table 1 is illustrated in Fig. 1, where the photographic reproductions have been ordered according to the orbital phase that will be discussed later.

The hydrogen and Fe II lines are the ones dominating the spectrum, as indicated in earlier publications. The main new features seen on our spectrograms are pure absorption lines due to He I: surprisingly this had never been reported earlier. Another new interesting feature is the occasional appearance of a second absorption component in the hydrogen lines. We further confirm the presence of the Balmer continuum as being in emission (Sanduleak and Stephenson, 1971; Gosset et al., 1984).

In the spectrum of GG Carinae the lines appear with different profiles according to the element involved. Figure 2 illustrates some types of profiles (density tracings) at the two different phases $\phi = 0.220$ and $\phi = 0.471$ (period $\simeq 31$ days, see later). As can be seen from parts *a* and *b* we confirm the Beals type III (Beals, 1951) P Cygni profile for the H lines. It is also possible to see in the spectra of part *b* the marked presence of the second absorption line. Figure 2c shows a typical Fe II line, λ4233: it is either a double or a very wide emission, whereas [Fe II] exhibits only single and fairly weak emission (see λ4287 in Fig. 2d). The region of Ca II K is rather complex (Fig. 2e): in addition to two emission wings that are readily visible (e_1, e_2) two faint absorption components labelled a_1 and a_3 seem to be present in the case of the K line only [Ca II H being severely blended with H_ε (see Fig. 2a)]; e_1 and e_2 seem to be from a large emission line (as in Fe II?) being strongly absorbed by a_2, the latter showing a shoulder in its blue wing at certain phases (see e.g. $\phi = 0.471$ in Fig. 2e). As clearly seen in Fig. 2f, whenever it is present He I is definitely in absorption with no emission component.

The positions of the lines have been determined either by measuring the "peak" (emission or absorption), or by adjusting the profile's envelope, i.e. by accurately superimposing the mirrored scans displayed on the measuring machine. In the case of hydrogen, five different features have been taken into account: they are labelled *a*, *b*, *c*, *d*, *e* in Fig. 2a and b, where: *a* refers to the

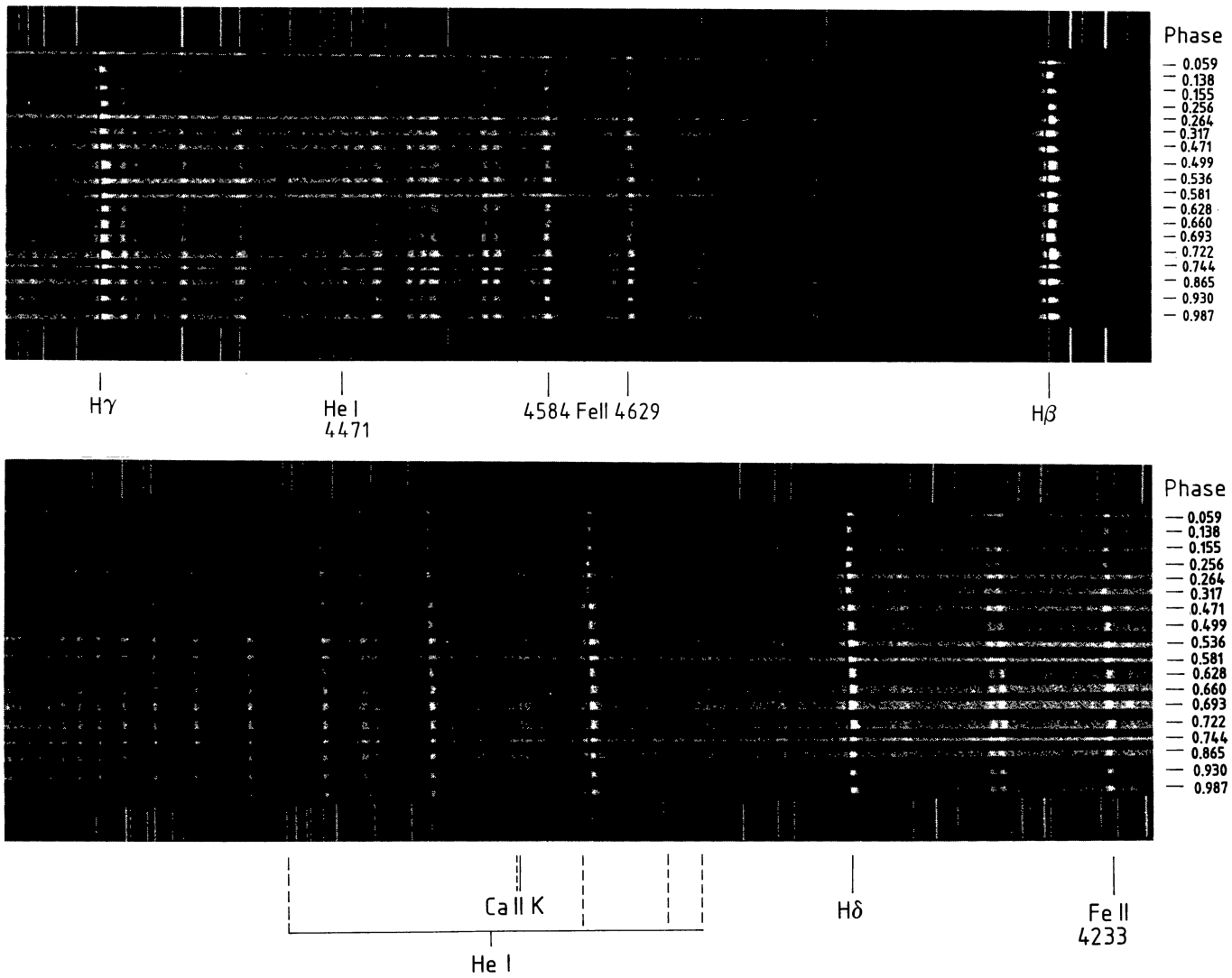

Fig. 1. Illustrative set of spectra of GG Carinae in the $\lambda 4330$–$\lambda 4870$ and $\lambda 3650$–$\lambda 4240$ wavelength regions (original dispersion: 12.3 Å mm^{-1}) obtained at the coudé focus of the ESO 1.52 m telescope (La Silla, Chile). The prints have been aligned with respect to the reference spectra and slightly displaced according to the solar velocity correction, in order to show the radial velocity evolution along one period. Phases are given to the right, on the basis of a 31.02 day period

envelope, *b* to the small emission that is sometimes present on top of the main emission component of the first Balmer lines (not visible in Fig. 2), *c* to the "blue" emission, *d* to the main absorption component, and *e* to the second absorption minimum (visible e.g. at $\phi = 0.471$, see Fig. 2b). The measurements were performed on the Grant machine of the European Southern Observatory (ESO) headquarters (Garching, FRG), and the reduction program called RAV at ESO was subsequently used to derive radial velocities. Although the r.m.s. accuracy of the fits and the repeatability of the measurements are of order 1 km s^{-1}, the "subjective" error in the choice of the line centroïd could be up to a factor ten larger. Table 2 lists the lines that have actually been measured.

4. The radial velocities along the light curve

4.1. Generalities

Before discussing each type of line (H, Fe II, [Fe II], Ca II, He I) separately in the following paragraphs, it is important to first point out the essential result of our study, namely that the radial velocities of most lines show a similar trend. This is definitely in favor of GG Carinae being a binary system. In fact the period derived from each line is always around 31 d: such a value disagrees with the one recommended by Gosset et al. (1984), which was twice as large. Because of the few points available along the period, one should stress that no precise period can actually be derived from the radial velocities. The best approach therefore is to take as a value for the period the single value computed by Gosset et al. (1984) on the basis of their extensive photometric data, i.e. $P = 31^{\mathrm{d}}.020$. The relevant mean lightcurve is illustrated in Fig. 3a for the *y* filter. At phase $\phi = 0$, one can see the primary minimum which now combines Min I and Min II (notation is from Gosset et al., 1984); slightly before $\phi = 0.5$ occurs the secondary minimum which was called Min III in the previous notation.

In the framework of a binary system, the radial velocities were subsequently analysed using the Wilsing-Russel method adapted for high eccentricities by Wolfe et al. (1967). The results of our "fits" are given in Table 3: columns 1 and 2 define the type of feature and the line(s) for which the data appear in columns 3

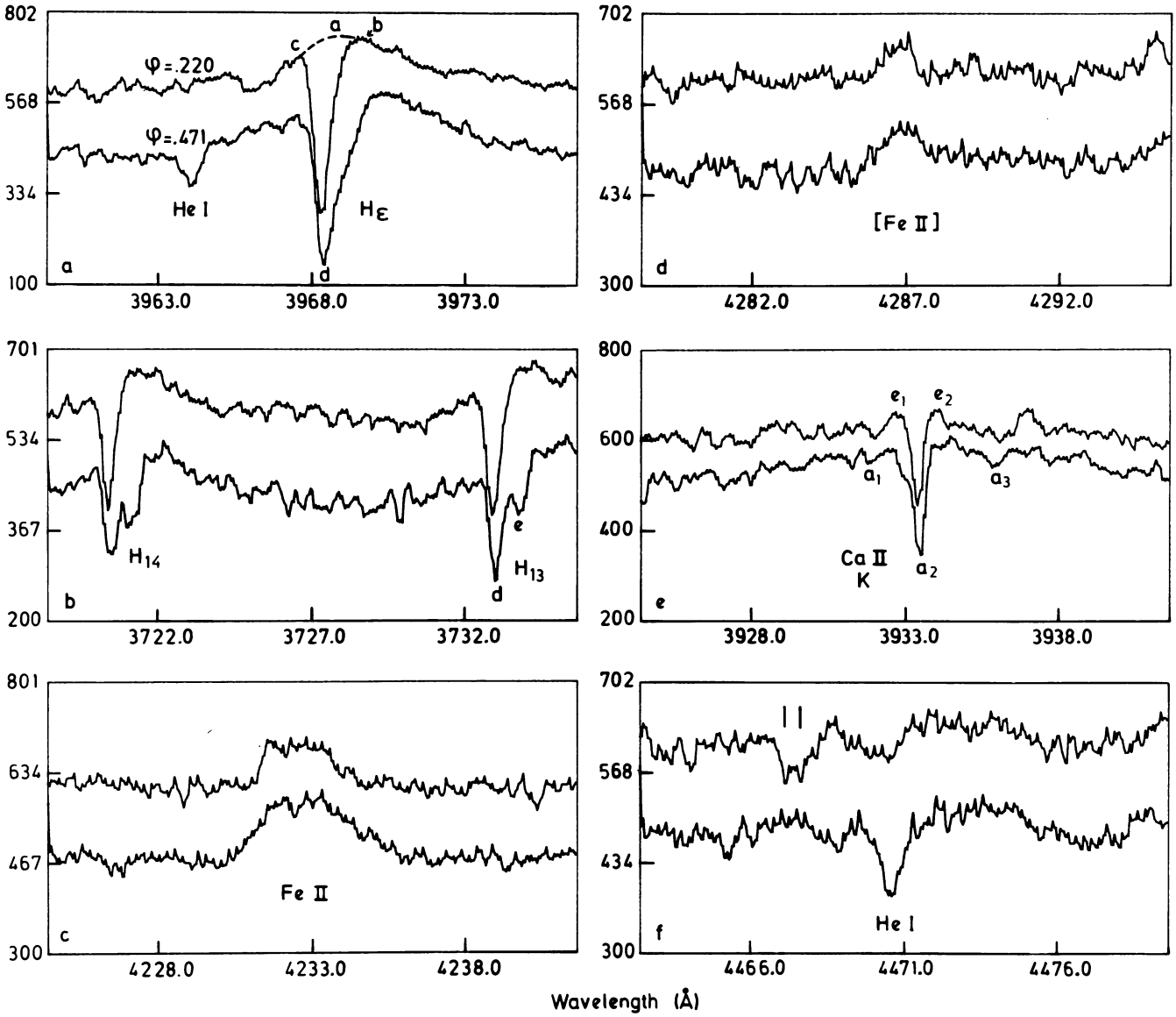

Fig. 2a–f. Line profiles at phases $\phi = 0.220$ (upper curve) and $\phi = 0.471$ (lower curve): **a** H_ε and He I λ3965; **b** H_{13} and H_{14}; **c** Fe II λ4233; **d** [Fe II] λ4287; **e** Ca II K line; **f** He I λ4471. Abscissae are wavelengths in Å and ordinates give arbitrary units. See text for description of each profile at different phases

(velocity of center of gravity V_0 or mean velocity $\overline{V}$ when the above mentioned method cannot be applied) and 4 (amplitude); columns 5–7 give the epoch of periastron, eccentricity, and longitude of periastron. For columns 3–7 the lower values in parentheses, which are aligned with the relevant digits, give the standard deviations.

4.2. *Hydrogen lines*

At all phases and without any effect related to the epoch, the variations of the radial velocity of the Balmer lines are a function of the excitation potential. For the emission lines there is an appreciable increase of the amplitude of the velocity variations (and of the dispersion) with n, up to H_{13}; in addition emissions with a large n seem to appear preferably between roughly phases 0.4 and 0.8. For the absorption lines the increase of the amplitude with n seems to exist, although much slower. The amplitudes (K) are $\simeq 20\,\mathrm{km\,s^{-1}}$ for H_γ, H_δ emissions, $\simeq 34\,\mathrm{km\,s^{-1}}$ for H_9, H_{10}, H_{11} emissions, and only 12 and 11 $\mathrm{km\,s^{-1}}$ for H_γ, H_δ and H_9, H_{10}, H_{11} absorptions, respectively. Figure 4 shows clearly that the average velocity of the H absorption lines is a function of the Balmer number n. So not only are the amplitudes a function of n, but also the average velocity of each H absorption. This latter phenomenon can of course be interpreted as an effect due to an outward accelerating envelope in which the P Cygni profiles are formed. The second absorption component of the Balmer lines appears essentially around phase $\phi = 0.45$, and may last up to $\phi = 0.65$.

As far as the orbital elements given in Table 3 are concerned, it is to be noted that they have been computed for several lines at once: for instance an average value for H_γ and H_δ is given in the table. These lines were chosen because H_β is not suitably located on IIa-O plates, and because H_ε and H_8 are contaminated by Ca II H and He I λ3888, respectively; H_9 through H_{11} have been used as well.

Figures 3b and c show the radial velocity curves for the Balmer emission lines, respectively $H_\gamma + H_\delta$, and $H_9 + H_{10} + H_{11}$.

Table 2. Lines measured in the spectrum of GG Carinae

H I	
Envelope	H_β to H_{19}
Small emission	H_β to H_δ
Blue emission	H_β to H_{19}
Absorption	H_β to H_{23}
Second absorption	H_ε to H_{19}
Fe II	
Multiplet 27	λλ4416.82, 4385.38, 4351.76, 4233.17, 4173.45 Å
Multiplet 28	λ4178.86 Å
Multiplet 37	λλ4629.34, 4555.89 Å
Multiplet 38	λλ4583.83, 4549.47 Å
Multiplet 42	λλ5018.43, 4923.92 Å
[Fe II]	
Emission	λ4287.40 Å
Ca II	
Emission and Absorption Components	K λ3933.66 Å
He I	
Absorption	λ4471.48 Å

4.3. Fe II *lines*

As indicated by Swings (1974) the Fe II lines are either broad with a central absorption, or double: what was measured here is the "envelope" of the entire profile (see Fig. 2c).

One may say that:

(i) with confidence, the amplitudes of the velocity variations in Fe II and in hydrogen (H_γ and H_δ) are identical (see Table 3);

(ii) the center of gravity velocity of Fe II is similar to that of hydrogen. In fact the Fe II emission mean velocities vary according to the multiplet involved (see Table 3);

(iii) there may exist a slight shift in phase between Fe II and H, of roughly 5 days: Fig. 3d shows the average curve for all measured Fe II lines.

4.4. [Fe II]

The only line that was measured is λ4287, the strongest [Fe II] line, which is single (Swings, 1974). This [Fe II] line roughly follows the overall motion along the light curve: the average velocity is similar to the center of gravity velocity of Fe II, and to that of H_γ and H_δ (see Table 3).

4.5. Ca II: *K line*

The Ca II H line being blended with H_ε, one may only use the K line which has a complex profile in the case of GG Carinae (see Sect. 3).

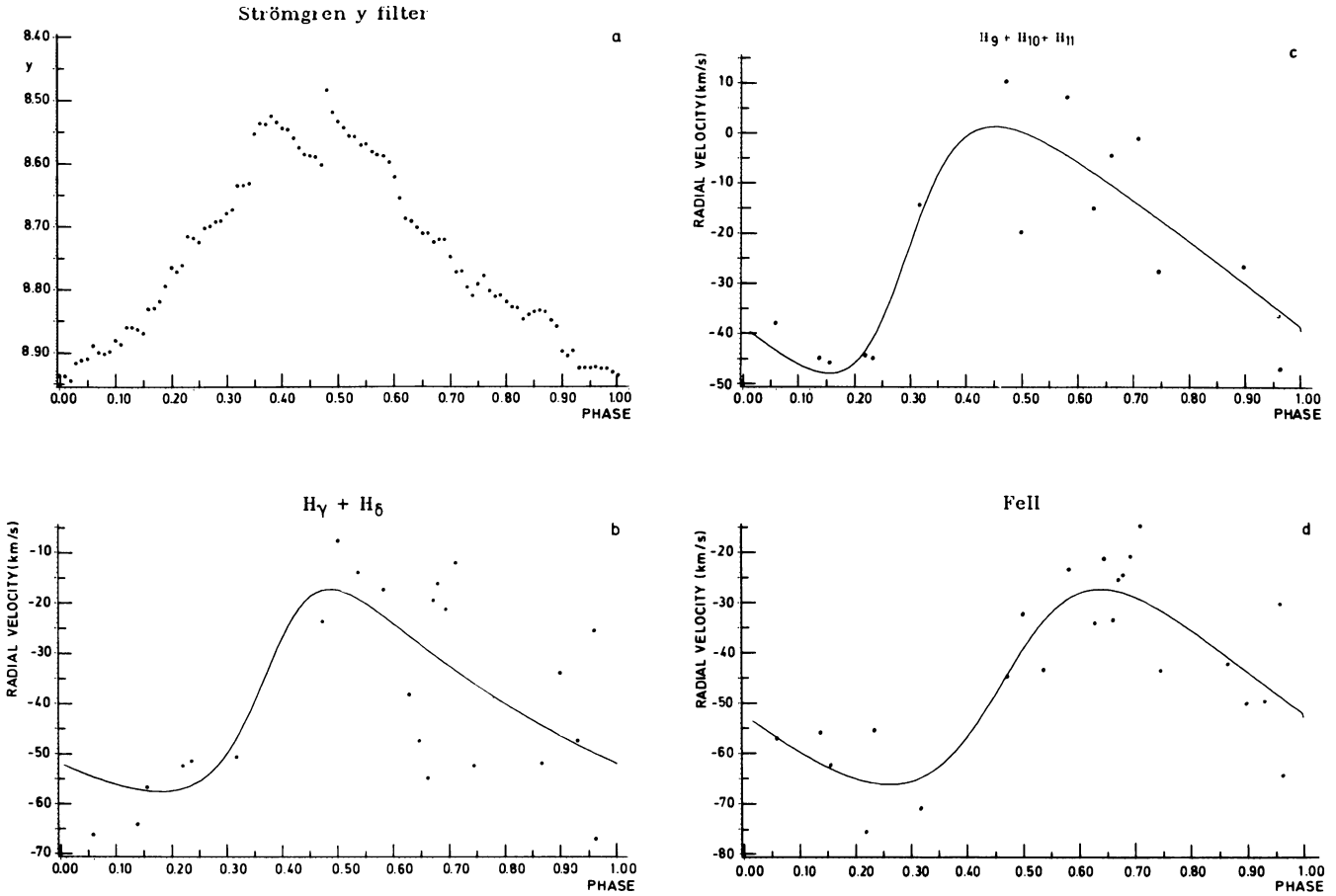

Fig. 3. **a** Light curve of GG Carinae in the Strömgren *y* filter (data from Gosset et al., 1984); **b–d** radial velocity variations of respectively $H_\gamma + H_\delta$; $H_9 + H_{10} + H_{11}$; and Fe II lines along a $31^d.02$ period. Dots represent the observations, while the continuous curve gives the result of the fit to the binary model (see text)

Table 3. Velocities, amplitudes and orbital data for GG Carinae

Type	Lines	V_0 or $\bar{V}$(a) (km s^{-1})	K (km s^{-1})	T:J.D. 2444000+	e	ω (°)
H envelope	$H_\gamma + H_\delta$	− 40.0 (3.7)	20.0 (5.4)	270.0 (4.0)	0.34 (0.16)	294 (41)
	$H_9 + H_{10} + H_{11}$	− 39.3 (4.8)	34.1 (5.9)	und.	und.	und.
H absorption	$H_\gamma + H_\delta$	−153.8 (2.3)	12.0 (2.0)	270.0 (2.0)	0.38 (0.34)	251 (50)
	$H_9 + H_{10} + H_{11}$	−142.4 (2.0)	11.0 (2.0)	269.0 (3.0)	0.24 (0.16)	236 (53)
H blue emission	$H_\gamma + H_\delta$	−226.0 (3.3)	13.0 (3.0)	und.	0.31 (0.27)	und.
H small emission	H_δ	− 22.6 (2.9)	24.3 (2.9)	269.0 (3.0)	0.33 (0.11)	264 (22)
H double absorption	$H_9 \rightarrow H_{14}$	− 99.0[b] (3.0)				
Fe II envelope	mult. 27–28	− 54.3 (2.2)	20.3 (3.5)	275.0 (2.0)	0.30 (0.15)	304 (28)
	mult. 37–38	− 46.5 (2.2)	17.6 (3.1)	275.0 (6.0)	0.24 (0.18)	304 (31)
	mult. 42	− 32.6 (2.7)	20.8 (4.0)	257.0 (3.0)	0.25 (0.18)	89 (30)
[Fe II] envelope	λ4287	− 47.7[a] (2.7)				
Ca II K	A1	−144.0[a] (3.0)				
	E1	− 87.3[a] (2.5)				
	A2	− 29.6 (1.4)	8.0 (2.0)	276.0 (3.0)	0.37 (0.25)	306 (39)
	E2	+ 27.0[a] (2.4)				
	A3	+151.0[a] (5.0)				
He I absorption	λ4471	−107.0[b] (14.0)				

[a] Mean velocity instead of V_0 because of very small amplitude K of the variations
[b] Mean velocity because line not present at all phases

It is only for the strong absorption component a_2 (see Fig. 2e) that some trustworthy results have been derived (see Table 3). Actually the value of -29.6 km s^{-1} derived for a_2 is quite similar to that of -23 km s^{-1} published by Hernandez et al. (1981), but could be of interstellar origin ... although, for our spectra, it is the only Ca II component having significant variations along the light curve! It is in fact interesting to note that a similar value is found in the case of the nearby peculiar object AG Carinae (Hutsemékers and Kohoutek, in preparation) as well as for more remote stars in the Carina nebula (see e.g. Walborn et al., 1984). It is not entirely clear that the two faint absorptions a_1 and a_3 do indeed belong to Ca II, since it is not possible to check whether similar features appear in the case of the Ca II H lines: a_1, however, seems to follow a trend similar to that of the hydrogen absorptions, while a_3 seems to behave differently from any other feature.

4.6. He I

The He I absorptions (λλ4471, 4026, 3965) appear at the same time as the second absorption component of the Balmer lines, i.e., as indicated earlier at certain phases (0.45 to 0.65). It should be stressed that we see no He I line in emission, but only absorption lines as reported in Sect. 3 (see e.g. Fig. 1). The He I lines do not seem to show any variation, although this fact is not necessarily significant because of the paucity of the data points (see also std.

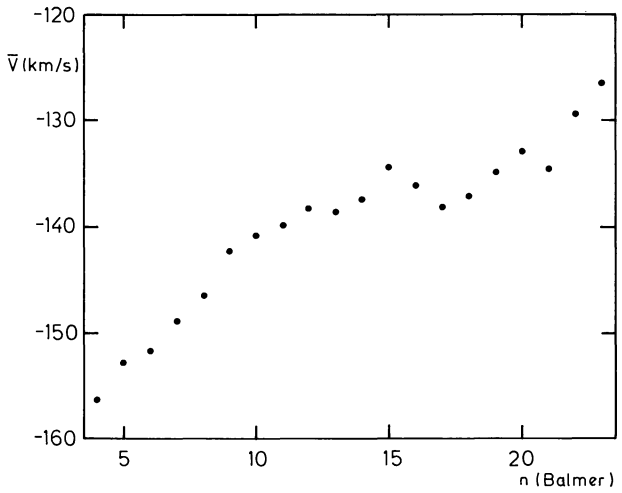

Fig. 4. Average velocity of the hydrogen absorption lines as a function of the Balmer number n (outward accelerating envelope)

deviation of 14 km s^{-1} in Table 3). The He I lines, however, will have to be kept clearly in mind when an attempt is made hereafter to sketch a physical model of the GG Carinae system.

5. Discussion

We have attempted to derive a physical model of GG Carinae on the basis of both the photometric data of Gosset et al. (1984) and the spectroscopic results described in the present paper.

It is to be said first that GG Carinae is undoubtedly a particular star or stellar system of which we will briefly summarize the main characteristics that are to be taken into account. Besides the permitted and forbidden emission lines the spectrum of GG Carinae exhibits P Cygni profiles for the Balmer lines during the whole light curve: they must originate near the object one sees, and produce an envelope around the primary star. As indicated previously, this envelope is accelerated outwards, and cannot be spherically symmetric but rather elongated or oddly shaped since the radial velocities show different variations from line to line (see Table 3). In addition there is a slight difference in phase between the Fe II and H radial velocity curves (see Fig. 3). Lines of higher excitation, i.e. the absorption lines of He I, as well as the second absorption component of the Balmer lines appear around phase $\phi \simeq 0.45$. As far as the light curve goes, it is worth recalling that it is composed of two minima that are different in width, so that a continuous variation must exist all along the period. Furthermore the variations in the u filter, although following those of v, b, and y, are much smaller, except at the time of a "glitch" (phase ~ 0.45) where the variations are similar (Gosset et al., 1984).

Before discussing GG Carinae as a binary system, it is worth pointing out that similarities to W Virginis type stars do exist, not only as far as the light curve is concerned, but also for spectroscopic characteristics, e.g. the presence of double hydrogen absorption lines and of double Fe II emissions at maximum light (see e.g. Abt, 1954).

Important differences exist however, e.g. for the radial velocity curve, and as far as the excitation goes (C IV, Si IV, etc. do indeed exist in absorption in the UV spectrum of GG Carinae, as seen on yet unpublished IUE data; not to mention the strong H emissions and the P Cygni profiles of the Balmer lines observed at all phases).

All in all it is thus believed that GG Carinae is not a single pulsating star, and that it is more appropriate to consider it as a peculiar binary system.

As mentioned in Sect. 4, the radial velocities have indeed been analyzed in terms of a binary system: the resulting orbital elements are given in Table 3, as computed for different lines. There results a mass function $M_2^3 \sin i/(M_1 + M_2)^2$ of order 0.02, indicating that the star we see is the most massive of the system.

Although we are not able to construct a physical model for GG Carinae that fits *all* the photometric and spectroscopic data, we nevertheless propose the following alternative in which the two models, having different characteristics but not excluding one another, qualitatively explain *most* of the data.

(i) GG Carinae, with its asymmetrical atmosphere in which the P Cygni profiles are formed, moves inside a very extended and dense "nebula", the continuous variation in brightness then being caused by extinction.

(ii) There exists a large hydrogen-rich hot spot on the companion of GG Carinae. A few unpublished data (narrow and large filters centred on H_α and H_β) show a well marked variation of H_α at the time of the partial occultation ("glitch"). In this case the light variation is caused by the orientation of the hot spot with respect to the observer. Could the GG Carinae system actually be a scaled down version of the enigmatic Of binary BD + 40°4220 (Cyg OB2 No. 5) of which a model was recently published by Vreux (1985, see his Fig. 6)?

In any case, for both models, it seems likely that it is at the time of periastron that we observe the "glitch" in the light curve, as well as the double H absorption components and the He I absorption lines: a partial occultation of the companion must thus take place at phase $\phi \simeq 0.45$, which implies an inclination of the GG Carinae system as seen from earth. It is also to be recalled that a mean eccentricity of about 0.3 has been derived for the system (see Table 3), and that the strong infrared excess which is observed is to be explained by a dust shell or important dust patches located either around GG Carinae itself or in the binary system.

GG Carinae thus remains an enigmatic and peculiar object: although a large amount of observational data exist, it is clear that more and better spaced (timewise) photometric and spectroscopic data are required in order to hope to "understand" GG Carinae. In addition, observations at the appropriate phase, in other wavelength regions (e.g. UV, X-ray) would most probably help in detecting, or not, the presence of a "hot spot".

References

Abt, H.A.: 1954, *Astrophys. J. Suppl.* **1**, 63
Allen, D.A.: 1973, *Monthly Notices Roy. Astron. Soc.* **161**, 145
Beals, C.S.: 1951, *Publ. Dom. Astrophys. Obs.* **9**, No. 1
Bouchet, P., Swings, J.P.: 1982, in *Be Stars*, IAU *Symp.* **98**, eds. M. Jaschek, H.G., Groth, p. 241
Cannon, A.J.: 1915, *Harvard Ann.* **76**, 31
Carlson, E.D.: 1968, Ph.D. Dissertation, Northwestern Univ.
Carlson, E.D., Henize, K.G.: 1979, *Vistas in Astron.* **23**, 213
Chen, K.Y., Kowalske, K., Austin, R.R.D.: 1983, *Publ. Astron. Soc. Pacific* **95**, 157
Cohen, M., Barlow, M.J.: 1980, *Astrophys. J.* **238**, 585
Gaposchkin, S.: 1953, *Harvard Ann.* **113**, No. 2
Garrison, R.F., Hiltner, W.A., Schild, R.E.: 1977, *Astrophys. J. Suppl.* **35**, 111
Garrison, R.F., Schild, R.E., Hiltner, W.A.: 1983, *Astrophys. J. Suppl.* **52**, 1

Gosset, E., Surdej, J., Swings, J.P.: 1984, *Astron. Astrophys. Suppl. Ser.* **55**, 411
Greenstein, N.K.: 1938, *Harvard Bull.* **908**, 25
Hernandez, C.A., Lopez, L., Sahade, J., Thackeray, A.D.: 1981, *Publ. Astron. Soc. Pacific* **93**, 747
Hoffleit, D.: 1933, *Harvard Bull.* **892**, 19
Hutsemékers, D., Kohoutek, L.: 1986 (in preparation)
Kruytbosch, W.E.: 1930, *Bull. Astron. Inst. Netherl.* **6**, 11
Pickering, E.C.: 1896a, *Astron. Nachr.* **141**, 169
Pickering, E.C.: 1896b, Harvard Circ., No. 9 (also *Astrophys. J.* **4**, 142)
Smith, H.J.: 1955, Southern Wolf-Rayet Stars, Ph.D. dissert., Harvard Univ.
Stephenson, C.B., Sanduleak, N.: 1971, Publ. Warner & Swasey Obs., Case Western Reserve Univ., Vol. I., No. 1
Swings, J.P.: 1974, *Astron. Astrophys.* **34**, 333
Vreux, J.M.: 1985, *Astron. Astrophys.* **143**, 209
Walborn, N.R., Heckathorn, J.N., Hesser, J.E.: 1984, *Astrophys. J.* **276**, 524
Wolfe, R.H., Jr., Horak, H.G., Storer, N.W.: 1967, Modern Astrophysics, Gauthier-Villars, Paris